

Bacterial attachment response to nanostructured titanium surfaces

Vi Khanh Truong¹, James Y. Wang², Wang Shurui³, Francois Malherbe¹, Christopher C. Berndt², Russell J. Crawford¹ and Elena P. Ivanova¹

¹Faculty Life and Social Sciences and ²Faculty of Engineering and Industrial Sciences, IRIS, Swinburne University of Technology

³Veeco Asia Pty Ltd

Corresponding address: Swinburne University of Technology, PO BOX 218, Hawthorn, Victoria, 3122, Australia.

Email: eivanova@swin.edu.au

Abstract— The effect of sub-nanometric surface roughness of Ti thin films surfaces on the attachment of two human pathogenic bacteria, *Staphylococcus aureus* CIP 65.8^T and *Pseudomonas aeruginosa* ATCC 9027, was studied. A magnetron sputtering thin film deposition system was used to control the titanium thin film thicknesses of 3 nm, 12 nm and 150 nm on silicon wafers with corresponding surface roughness parameters of R_q 0.14 nm, 0.38 nm and 5.55 nm ($1 \mu\text{m} \times 1 \mu\text{m}$ scanning area). Analysis of bacterial retention profiles showed that the bacteria responded differently changes in the R_a and R_q (Ti thin film) surface roughness parameters of a less than 1 nm, with up to 2 - 3 times: more cells being retained on the surface, and elevated levels of extracellular polymeric substances being secreted on the Ti thin films, in particular on the surfaces with 0.14 nm (R_q) roughness.

Keywords: sub-nanometric surface morphology, bacterial attachment, titanium

I. INTRODUCTION

Titanium has become the most popular metal for the construction of biomedical devices including orthopedic and dental prostheses and cardiac valves, maxiofacial surgery and vascular stents, due to its high biocompatibility, low toxicity and high corrosion resistance [1, 2]. The use of these implants is increasing and diversifying, as is research into the use of titanium with bioactive surface modifications to increase biocompatibility [3].

Biofilm formation of pathogenic bacteria on implant materials has been connected with resulting infections. These can be dramatically harmful, leading to the necessity to remove the devices. These infections can also be associated with systemic infection, loss of function, and in extreme cases, amputation or death [3-5]. It has also been well documented that the formation of bacterial biofilms can significantly increase resistivity against antimicrobial substances [6, 7]. For example, Troodle et al., showed that biofilms of *S. aureus*, *E. coli* and *P. aeruginosa* were present on all samples collected from catheters removed from patients, despite the fact that disinfection processes being employed [8]. *S. aureus* strains, in particular, have been reported as significant contributors to infections associated with orthopedic implants [9], and therefore an thorough

understanding of the attachment characteristics of *S. aureus* to host tissues and inanimate surfaces is critical in efforts to reduce infection.

II. MATERIAL AND METHODS

A. Titanium thin films preparation

Titanium thin films of 3 nm, 12 nm or 150 nm thickness (henceforth referred to as 3 nm, 12 nm or 150 nm films) were prepared using pre-cleaned silicon (100) wafers using a Kurt J Lesker CMS -18 magnetron sputtering thin film deposition system as previously described [10].

B. Titanium thin film characterisation

The sessile drop method was used to measure the contact angles of different solvents on titanium surfaces [11]. Three solvents, MilliQ water, formamide (Sigma) and diiodomethane (Sigma) were used. An FTA1000c (First Ten Ångströms Inc.) instrument equipped with a nanodispenser was used to measure the contact angles at room temperature (ca 23°C) in air.

A scanning probe microscope (SPM) (Innova, Veeco) was used to image the surface morphology and to quantitatively measure and analyze the surface roughness of the metallic surfaces on the nanometer scale. The analysis was performed in the tapping mode as it minimizes the interaction between tip and sample and thus can avoid the destructive action of lateral forces that exist in contact mode.

The surface composition of the titanium-coated glass slides were determined from X-ray photoelectron spectra using a Kratos Axis Ultra DLD spectrometer (Kratos Analytical Ltd, U.K.). Spectra were recorded while irradiating the samples with a monochromatic Al K α source ($h\nu = 1486.6$ eV) operating at 150W. The analysis area was approximately $300 \mu\text{m}^2 \times 700 \mu\text{m}^2$.

C. Bacterial strains

The bacteria used in this study were *Staphylococcus aureus* CIP 65.8 and *Pseudomonas aeruginosa* ATCC 9027. Bacterial strains were obtained from American Type Culture

Collection (ATCC, USA) and Culture Collection of the Institute Pasteur (CIP, France).

Prior to each experiment, a fresh bacterial suspension was prepared for each of the strains grown overnight in 100 mL of nutrient broth (Oxoid) (in 0.5 L Erlenmeyer flasks) at 37 °C with shaking (120 rpm). All bacterial cell suspensions were prepared as previously described with $OD_{600} = 0.3$ [10]. An aliquot of 5 mL of bacterial suspension was added in a sterile Petri-dish with samples of titanium films and allowed to incubate for 18 h at room temperature (ca. 22°C). Sterile nutrient broth (5 mL) was used as a negative control. Samples were handled under sterile conditions until just prior to imaging as described elsewhere [10]

D. Visualization and quantification of viable cells and EPS

High-resolution images of titanium thin films with the retained bacterial cells were taken using an FESEM (ZEISS SUPRA 40VP) at 3 kV. Images with 5,000× magnification were used to calculate the number of bacteria adhering to the titanium surfaces; the results were statistically analyzed. Three independent experiments were carried out and for each experiment, six SEM fields of view were used to calculate the number of retained bacteria.

In order to visualize viable bacteria and the EPS, standard staining techniques were used. Thus, viable bacteria were stained with SYTO® 17 Red (Molecular Probes™, Invitrogen) and the EPS was stained green with Alexa Fluor® 488 (Molecular Probes™, Invitrogen), a conjugate of succinylated concanavalin A [12-14]. Images of the bacteria attached to titanium surfaces and the EPS were recorded with a confocal scanning laser microscope (CSLM) Olympus Fluorview FV1000 Spectroscopic Confocal System. The imaging software Fluorview FV 7.0 was employed to process the CSLM images and construct 3D images.

III. RESULTS AND DISCUSSION

A. Ti film surface characteristics

A comparative AFM analysis of the titanium thin films indicated an increase in the surface roughness parameters at the nano-metre scale as the thickness of the Ti layer was increased (Fig. 1 and Table I). The bare silicon wafer exhibited the smoothest surface, with an R_q of 0.11 nm.

The progression of the surface roughness parameters and change in surface morphology is best seen in the images presented in Fig. 1, and in the data presented in Table 1. The degree of roughness associated with the silicon wafer substrate was accentuated by the titanium sputtering: a 3 nm film of titanium produced heterogeneous smoothness with dense nano-peaks and valleys. Due to the sub-nanometric smoothness and homogeneous surface characteristics of the silicon wafer, the initial roughness of the 3 nm Ti surfaces is unlikely to be affected by the shadow effect associated with the sputtering process [10]. Apart from the commonly used surface roughness parameters, e.g. R_a , R_q and R_{max} , skewness (R_{skw}) and kurtosis (R_{kur}) were used as additional surface roughness parameters to all the full surface characterization of the surface morphology. As the evolution of R_{skw} values clearly demonstrates in Fig. 1, increasing film thicknesses

appears to induce more heterogeneity in the surface morphology.

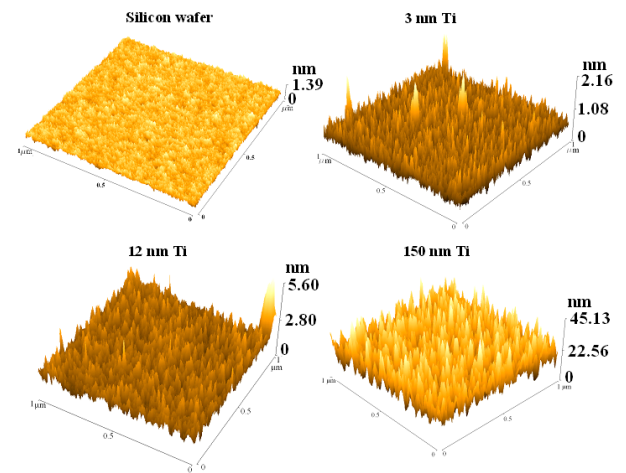


Figure 1. Typical 3D AFM images (1 $\mu\text{m} \times 1 \mu\text{m}$ scanning areas) of the silicon wafer; 3 nm, 12 nm and 150 nm Ti thin films thicknesses on silicon wafers.

TABLE I. AFM SURFACE ROUGHNESS ANALYSIS OF Ti THIN FILM SURFACES

Ti film thicknesses (nm)	0 nm	3 nm	12 nm	150 nm
Average roughness R_a	0.14 ± 0.01	0.13 ± 0.01	0.28 ± 0.03	4.42 ± 0.44
RMS roughness R_q	0.11 ± 0.01	0.14 ± 0.01	0.38 ± 0.04	5.55 ± 0.56
Maximum height R_{max}	1.54 ± 0.15	2.16 ± 0.22	5.60 ± 0.56	43.20 ± 4.32
Skewness R_{skw}	0.07	0.30	0.31	0.34
Kurtosis R_{kur}	3.10	3.31	3.34	3.13

The XPS elemental analysis was carried out for both Ti thin films and silicon wafers to assess the surface elemental composition, chemical functionality and Ti coverage of each film. These analyses showed that titanium and oxygen were the most abundant elements, indicating that Ti was present as TiO_2 . Slightly lower atomic fractions of Ti were found on the 3 nm and 12 nm film surfaces than on the 150 nm film surface, this likely being due to the heterogeneity of the Ti films as a consequence of the nano-roughness of silicon wafers (Table II). The depth of XPS analysis varies with the nature of the surface, but is typically around 5 nm to 10 nm. Thus, for a perfectly flat interface between the silicon wafer and Ti, one would expect the Si:Ti ratio to progressively decrease until the depth of the Ti layer became greater than the depth of analysis, which is indeed demonstrated in this case. It appeared that 8.5 % of silicon was detected on 3 nm Ti surfaces and 0.1 % of silicon was detected on 12 nm Ti surfaces.

TABLE II. ATOMIC FRACTIONS OF ELEMENTS DETECTED ON THE SURFACE OF EACH SAMPLE BY XPS

Ti film thickness [nm]	O	Ti	N	C	Si
0	38.3	<dl	0.5	8.0	53.3
3	46.3	17.7	1.7	25.6	8.5
12	46.0	18.7	2.1	33.0	0.1
150	48.8	21.7	2.3	27.1	<dl

The 150 nm films were found to be highly hydrophobic ($\theta_w = 104.5^\circ$), while the 3 nm and 12 nm films were found to be less hydrophobic ($\theta_w \sim 97^\circ$). The difference in contact angles is regarded as statistically significant between 3 nm and 150 nm; 12 nm and 150 nm Ti surfaces (t -test: $p = 0.03$ (<0.05)). Surface free energies of polar components on 3, 12 and 150 nm Ti surfaces were in the range of 35.0 mN m^{-1} and 39.5 mN m^{-1} .

B. Bacterial attachment on Ti films

The analysis of SEM and CSLM images (Fig. 2) indicated that *P. aeruginosa* and *S. aureus* exhibited varying attachment responses when grown on the titanium surfaces used in this study. Overall, *S. aureus* were capable of successfully colonizing the subnano-smooth titanium surfaces whereas *P. aeruginosa* appeared to be a poor colonizer of the same surfaces.

The number of *P. aeruginosa* cells attached (Table III and Fig. 2) onto the 3 nm and 12 nm Ti surfaces were shown to be statistically insignificantly different ($t = 0.84, p > 0.05$), while the number of *P. aeruginosa* cells attached on 3 nm and 12 nm Ti surfaces were found to be statistically significantly more than that found on the 150 nm Ti surfaces (Table III) ($t = 0.01$ and 0.04 respectively, $p < 0.05$). Production of EPS was greater on the 3 nm and 12 nm Ti

surfaces compared with the 150 nm Ti surfaces (Fig. 2).

TABLE III. NUMBERS OF RETAINED CELLS ON 3 nm, 12 nm AND 150 nm TITANIUM SURFACES ON SILICON WAFERS

Bacterial strain	Retained cells $\times 10^5$ [number of cells per mm^2]		
	Titanium thicknesses (nm)		
	3	12	150
<i>P. aeruginosa</i>	2.71 ± 0.69	2.82 ± 0.78	1.74 ± 0.43
<i>S. aureus</i>	22.44 ± 3.40	19.81 ± 4.66	11.66 ± 1.54

There was no statistically significant difference in the number of *S. aureus* cells attaching to the 3 nm and 12 nm Ti surfaces, ($t = 0.28, p > 0.05$) (Fig. 2). CLSM images of viable cells (colored red) and EPS production (colored green) confirmed the attachment pattern *S. aureus* cells on 3 nm and 12 nm Ti surfaces. The number of *S. aureus* cells attached on the subnano-metric smooth 3 nm and 12 nm Ti surfaces was therefore greater than that on 150 nm Ti surfaces (confirmed by statistical analysis ($p = 0.001$ and 0.006 respectively, $t < 0.01$). The results of this study are in agreement with our current investigations of the bacterial responses to changes in nano-topography of glass, polymer surfaces and ultra-fine grain Ti surfaces, thus confirming the hypothesis that nano-topographic surface morphology and topography strongly influence the degree of bacterial attachment to surfaces [15-17].

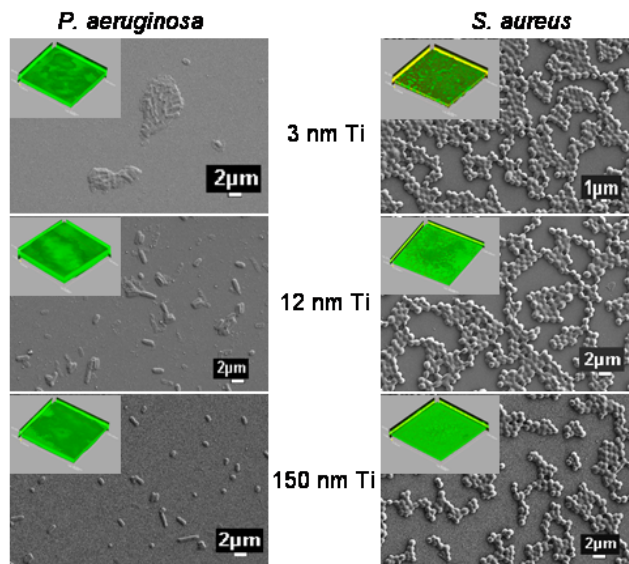


Figure 2. Typical SEM image of *P. aeruginosa* (left) and *S. aureus* (right) attachment on 3 nm, 12 nm and 150 nm Ti films on silicon wafers. Typical CLSM images of *P. aeruginosa* (top) and *S. aureus* (top) EPS on 3 nm, 12 nm and 150 nm Ti films on silicon wafers (with scanning areas $126 \mu\text{m} \times 126 \mu\text{m}$).

IV. CONCLUSION

The controlled deposition of titanium onto silicon wafers resulted in the fabrication of surfaces with differing morphology with subnano-roughness topographic features, which controlled the overall surface architecture. Remarkably, the extent of attachment of *P. aeruginosa* and *S. aureus* indicated that they had the ability to differentiate between surfaces with very small differences in surface roughness, of the order of about 0.14 nm - 5.5 nm (R_q parameters). The attachment of *P. aeruginosa* and particularly *S. aureus* to titanium is of considerable importance to the fabrication of medical implants.

ACKNOWLEDGEMENT

This study was supported in part by Advanced Manufacturing Co-operative Research Centre (AMCRC). V. K. T. is a recipient of Swinburne University Postgraduate Research Award (SUPRA) award.

REFERENCES

- [1] K. A. Whitehead, and J. Verran, "The effect of surface properties and application method on the retention of *Pseudomonas aeruginosa* on uncoated and titanium-coated stainless steel," *International Biodeterioration & Biodegradation*, 60, 74-80 (2007).
- [2] Y. L. Jeyachandran, B. Karunakaran, S. K. Narayandass et al., "Properties of titanium thin films deposited by dc magnetron sputtering," *Materials Science and Engineering A*, 431, 277-284 (2006).
- [3] M. C. Hudson, W. K. Ramp, and K. P. Frankenburg, "*Staphylococcus aureus* adhesion to bone matrix and bone-associated biomaterials," *FEMS Microbiology Letters*, 173, 279-284 (1999).
- [4] Y. L. Ong, A. Razatos, G. Georgiou et al., "Adhesion forces between *E. coli* bacteria and biomaterial surfaces," *Langmuir*, 15, 2719-2725 (1999).
- [5] C. Diaz, M. C. Cortizo, P. L. Schilardi et al., "Influence of the nano-micro structure of the surface on bacterial adhesion," *Materials Research*, 10, 11-14 (2007).
- [6] R. M. Donlan, "Biofilm formation: A clinically relevant microbiological process," *Clinical Infectious Diseases*, 33, 1387-1392 (2001).
- [7] Y. H. An, R. J. Friedman, R. A. Draughn et al., "Rapid quantification of staphylococci adhered to titanium surfaces using image analyzed epifluorescence microscopy," *Journal of Microbiological Methods*, 24, 29-40 (1995).
- [8] L. Troidle, and F. Finkelstein, "Treatment and outcome of CPD-associated peritonitis," *Annals of Clinical Microbiology and Antimicrobials*, 5, 1-7 (2006).
- [9] G. J. Tortora, B. R. Funke, and C. L. Case, *Microbiology: An Introduction*, 8th ed., San Francisco: Pearson Education Inc, Benjamin Cummings, 2004.
- [10] E. P. Ivanova, V. K. Truong, J. Wang et al., "Impact of Nanoscale Roughness of Titanium thin films surfaces on Bacterial Retention," *Langmuir*, 26, 1973-1982 (2010).
- [11] D. Öner, and T. J. McCarthy, "Ultrahydrophobic surfaces. Effects of topography length scales on wettability," *Langmuir*, 16, 7777-7782 (2000).
- [12] N. Mitik-Dineva, J. Wang, R. C. Mocanasi et al., "Impact of nanotopography on bacterial attachment," *Biotechnology Journal*, 3, 536-544 (2008).
- [13] R. Maeyama, Y. Mizunoe, J. M. Anderson et al., "Confocal imaging of biofilm formation process using fluoroprobed *Escherichia coli* and fluoro-stained exopolysaccharide," *Journal of Biomedical Materials Research - Part A*, 70, 274-282 (2004).
- [14] Y. V. Nancharaiyah, V. P. Venugopalan, S. Wuertz et al., "Compatibility of the green fluorescent protein and a general nucleic acid stain for quantitative description of a *Pseudomonas putida* biofilm," *Journal of Microbiological Methods*, 60, 179-187 (2005).
- [15] N. Mitik-Dineva, J. Wang, V. K. Truong et al., "*Escherichia coli*, *Pseudomonas aeruginosa* and *Staphylococcus aureus* attachment patterns on glass surfaces with nanoscale roughness," *Current Microbiology*, 58, 268-273 (2009).
- [16] E. P. Ivanova, N. Mitik-Dineva, J. Wang et al., "*Staleyia guttiformis* attachment on poly(tert-butylmethacrylate) polymeric surfaces," *Micron*, 39, 1197-1204 (2008).
- [17] V. K. Truong, R. Lapovok, Y. Estrin et al., "The influence of nanoscale surface roughness on bacterial adhesion to ultrafine-grained titanium," *Biomaterials*, 31, 3674-3683 (2010).